OPTIMIZATION OF NEUROMUSCULAR ELECTRICAL STIMULATION TO REDUCE MUSCLE FATIGUE DURING ISOMETRIC CONTRACTIONS

by

Brian D. Doll

B.S. in Electrical Engineering, University of Tennessee, 2010

Submitted to the Graduate Faculty of

Swanson School of Engineering in partial fulfillment

of the requirements for the degree of

Master of Science

University of Pittsburgh

2015

UNIVERSITY OF PITTSBURGH

SWANSON SCHOOL OF ENGINEERING

This thesis was presented

by

Brian D. Doll

It was defended on

April 3, 2015

and approved by

Nitin Sharma, Ph.D. Assistant Professor,

Department of Mechanical Engineering and Materials Sciences

Amro El-Jaroudi, Ph.D. Associate Professor,

Department of Electrical and Computer Engineering

Ervin Sejdic, Ph.D. Assistant Professor,

Department of Electrical and Computer Engineering

Thesis Advisors: Nitin Sharma, Ph.D. Assistant Professor,

Department of Mechanical Engineering and Materials Sciences,

Zhi-Hong Mao, Ph.D. Associate Professor,

Department of Electrical and Computer Engineering

OPTIMIZATION OF NEUROMUSCULAR ELECTRICAL STIMULATION TO REDUCE MUSCLE FATIGUE DURING ISOMETRIC CONTRACTIONS

Brian D. Doll, M.S.

University of Pittsburgh, 2015

The objective of this Thesis is to show that a neuromusclar model can be used to calculate an optimized train that will impede the onset of muscle fatigue while tracking a pre-defined force reference. Implementation of a predictive force and fatigue model of a human skeletal muscle when stimulated with neuromuscular electrical stimulation (NMES) is presented herein. In this implementation, the nonlinear model is used to control muscle force to a reference. Muscle control is optimized in such a way that muscle fatigue is minimized, demonstrating potential for improvements in applications where NMES use is limited by muscle fatigue. Model parameters were identified for the able-bodied subjects and testing was performed to identify the response of the muscle to a constant frequency stimulation. An optimization algorithm was then used to compute a pulse train that will maintain an isometric contraction at a constant force for a period of time without unnecessarily fatiguing the muscle. Following each train, the fatigue of the muscle was evaluated to determine if muscle fatigue was reduced. The study has concluded that muscle fatigue was significantly reduced when an optimized train is used when compared to a constant frequency train.

TABLE OF CONTENTS

LIST OF TABLES

LIST OF FIGURES

1.0 INTRODUCTION

Functional electrical stimulation (FES) is commonly used to induce voluntary-like contractions in skeletal muscles through application of low-level electrical pulses. FES can assist individuals with mobility impairments to achieve functional tasks such as standing and walking [28], drop foot correction [20], grasping [25, 26], and bladder control [24]. However, application of FES is limited by the rapid onset of muscle fatigue.

Factors such as the stimulation method, muscle fiber composition, state of training of the muscle, and task to be performed have been observed to affect fatigue during neuromuscular electrical stimulation (NMES), which is the clinical application of FES where it is used to treat muscle atrophy. Researchers have proposed different stimulation strategies to delay the onset of fatigue such as choosing stimulation frequency and pattern, sequential stimulation, and size order recruitment. During NMES, constant frequency trains (CFT) are generally used to activate skeletal muscles. Recently, variable frequency trains (VFT) and doublet frequency trains (DFT) have been shown to significantly improve the force production from the fatigued muscles [12]. The CFT is a pulse train with equally spaced single pulses; the DFT is a pulse train with doublet pulses spaced equally; and the VFT is a CFT with a doublet for the initial pulse (see Fig. 1).

Among numerous muscle models, this Hill/Huxley-type model is one of the few muscle models that can accommodate a variety of stimulation trains. In an experimental comparison made by [18], the Hill/Huxley-type nonlinear model predicted muscle force time profiles most accurately. The other models considered in the comparison were a second-order nonlinear model proposed by Bobet and Stein [5] and a simple linear differential equation relating force with stimulation trains modeled as Dirac delta functions [18]. The Hill/Huxley nonlinear model has been shown to predict muscle response for a wide range of frequencies and pulse

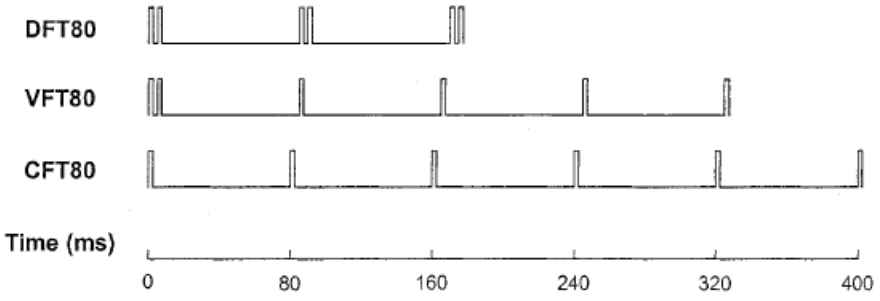

Figure 1: Stimulation patterns as investigated in [9–11](republished from [11])

patterns (CFT, DFT, and VFT) [9–11]. Because this model can predict muscle force based on individual pulse times, changes in stimulation frequency are already considered in the model making it ideal for this application where the stimulation frequency will be continually changing to account for muscle fatigue. The model was successfully used to predict optimal stimulation trains that produce force-time integrals comparable to CFT while inducing less muscle fatigue.

The objective is to determine optimized stimulation patterns based on a mathematical model that can predict skeletal muscle forces and fatigue in response to electrical stimulation. This would enable NMES systems to deliver custom stimulation patterns that produce a desired muscle force while delaying the onset of muscle fatigue. The purpose of this thesis is to demonstrate a method of NMES pulse train optimization that will track a pre-defined force reference and limit muscle fatigue. The optimization is performed by minimizing a cost function that contains both the predicted error from the force reference and the number of stimulation pulses in the delivered train.

The results suggest that this model performs sufficiently well to be implemented for use in a model-based control scheme. The key contribution of this thesis is that the muscle fatigue was shown to be lower when the optimized stimulation pulse train was delivered in comparison to a constant frequency train. This thesis contains discussion on how parameters for the model were identified, how these parameters were used to define an optimized pulse train, and how muscle fatigue caused by a computed optimized pulse train compares to muscle fatigue caused by a constant frequency train.

2.0 BACKGROUND

2.1 HISTORY OF NMES MUSCLE RESPONSE MODELING

Although NMES is commonly used in clinical applications, the force response of the muscle, specifically as it relates to muscle fatigue, is only partially understood. Electrical stimulation of muscle tissue has been investigated by Hodgkin and Huxley since as early as 1939 [15]. Early medical applications of muscle stimulation were studied for use in cardiac patients [30] and drop foot correction [19]. As this research expanded, the application of electrical stimulation to produce non-voluntary muscle contractions became know as functional electrical stimulation [22].

Investigations into the input-output relationship of the skeletal muscle were presented by Hill in 1938 [14]. This work resulted in a muscle model based on the force mechanics of the muscle. The work presented in [14] models the muscle similar to a spring and damper-type systems. Although this model was not initially implemented in studies of electrical muscle stimulation, the actin and myosin cross-bridges incorporated into modern NMES models are based on this work. [29]

Huxley-type models, which expanded from the initial work in [15] are action potential based muscle models that rely upon ion channel behaviour in the muscle. [6, 16] The relationship between Ca^{2+} and the force generated by the muscle were first investigated in the Huxley-type models and this is the portion of the model that was incorporated into many modern models [16, 29].

Later investigations of surface electrode NMES applications included maintaining posture in paraplegic patients [17], muscle exercise in paralyzed subjects [23], and NMES assisted walking [21, 27]. As control complexity of these tasks increases, the need for an effective muscle model is realized. Early muscle models were developed by Bernotas et al. [3], Binder-Macleod et al. [7], Bobet and Stein [5], and Dorgan and O'Malley [13]. The Hill-Huxley-type model(specifically the Binder-Macleod Model) [7] and the Bobet and Stein model [5] are the two isometric muscle force models best known and most applied today. Further detail is presented on these models in the Section 2.2.

2.2 DISCUSSION OF RECENT ISOMETRIC MUSCLE FORCE MODELS

2.2.1 The Bobet and Stein Model

The model proposed by Bobet and Stein [5] is presented as follows:

$$q(t) = \int \exp(-aT)u(t-T)dT, \tag{2.1}$$

$$x(t) = \frac{q(t)^n}{q(t)^n + k^n}, \tag{2.2}$$

$$F(t) = Bb \int \exp(-bT)x(t-T)dT, \tag{2.3}$$

$$b = b_0 \left(1 - \frac{b_1 F(t)}{B}\right)^2 \tag{2.4}$$

The model comprises of a set of two first order differential equations, a saturation equation, x, and a rate factor of force, b, which also varies as a function of force. In Equations 2.1-2.4, a, B, b_0, b_1, n, and k are constant, pre-identified muscle parameters to control force force, F [18]. This model accounts for muscle fatigue by describing the system dynamics on a large scale as a function of how they change over time.

2.2.2 The Ding et al. Model

The early implementation of the Ding et al. model [7] did not include any compensation for muscle fatigue. The Ding et al. Model is a Hill-Huxley model of muscle stimulation, meaning that it derives components from the works of both popular muscle models [29]. This model was initially presented as follows:

$$\frac{dC_N}{dt} = \frac{1}{\tau_c}\sum_{i=1}^{n}\exp\left(-\frac{t-t_i}{\tau_c}\right) - \frac{C_N}{\tau_c}, \tag{2.5}$$

$$\frac{dF}{dt} = A\frac{C_N}{K_m + C_N} - \frac{F}{\tau_1 + \tau_2\frac{C_N}{K_m+C_N}}. \tag{2.6}$$

Muscle parameters for this model are defined in Table 1. The model consists of 2 differential equations but is not particularly useful because each type of pulse train requires re-parameterization of the model. The model was later augmented to add a scaling factor, R_i to account for for the effect of previous pulses and additional components for force-based muscle fatigue and time-based muscle recovery modeling [8, 12].

Table 1: Definition of early Ding et al muscle model parameters (Adapted from [11])

Symbol	Definition
A	Scaling factor for the force and the shortening velocity of the muscle
C_N	Representation of Ca^{2+}-troponin complex
F	Instantaneous force
t_i	Time of the i^{th} stimulation
τ_1	Time constant of force decline at the absence of strongly bound cross-bridges
τ_2	Time constant of force decline due to the extra friction between actin and myosin resulting from the presence of cross-bridges.

A later version of the model, presented by Ding et al. in 2000 is as follows: [12]

$$\frac{dC_N}{dt} = \frac{1}{\tau_c}\sum_{i=1}^{n}R_i\exp\left(-\frac{t-t_i}{\tau_c}\right) - \frac{C_N}{\tau_c},$$

$$R_i = 1 + (R_0 - 1)\exp[-(t_i - t_{i-1})/\tau_c], \tag{2.7}$$

$$\frac{dF}{dt} = A\frac{C_N}{1+C_N} - \frac{F}{\tau_1 + \tau_2\frac{C_N}{1+C_N}}.$$

Later in 2000, the muscle fatigue model was presented by Ding et al. as follows: [8]

$$\begin{aligned}
\frac{dA}{dt} &= -\frac{A - A_{rest}}{\tau_{fat}} + \alpha_A F, \\
\frac{dR_0}{dt} &= -\frac{R_0 - R_{0,rest}}{\tau_{fat}} + \alpha_{R_0} F, \\
\frac{d\tau_1}{dt} &= -\frac{\tau_c - \tau_{1,rest}}{\tau_{fat}} + \alpha_{\tau_c} F.
\end{aligned} \tag{2.8}$$

Later works further updated the model to include a K_m term [9, 10], which controls the sensitivity of the force to changes in C_N and to replace R_0 in the fatigue model with K_m [11]. The most recent version of the model, presented in 2003 [11], was used for the research described in this thesis and is presented in Chapter 4. All muscle parameters for these models are described in Table 2.

3.0 THE PROBLEM OF NMES-INDUCED MUSCLE FATIGUE

NMES application is limited by the rapid onset of muscle fatigue. The onset of fatigue is more rapid when using surface NMES stimulation than for a similar voluntary contraction because NMES recruits motor units in a non-selective, spatially fixed, and temporally synchronous pattern, compared to the voluntary recruitment in which motor units are asynchronously activated at lower frequencies [4].

Muscle fatigue is defined as a decline in the force of a muscle contraction due to muscle activity [1]. Effective fatigue management is very relevant to NMES applications because it is always desirable to maintain muscle force for a longer period of time. Force production is directly related to the flow of calcium in the muscle and resistance to muscle fatigue is a reflection of changes in the calcium dynamics as the muscle is recruited [2]. Based on the fatigue model presented by Ding et al. [9–11], the magnitude of force generation is the only independent variable that predicts muscle fatigue. Muscle recovery is predicted based on time. The problem therfore, is that muscle recruitment must be limited to only what is necessary to complete a desired task. Constant frequency pulse trains do not address this issue because the force generated varies as the muscle fatigues. The design of stimulation patterns to account for NMES induced fatigue is not well investigated.

The task therefore, is to design a method to generate custom stimulation patterns that produce a desired muscle force and do not overly-fatigue the muscle. This will be accomplished by using optimization to define a stimulation pulse train that will allow sufficient time between pulses for the muscle to recover, and avoid excess force generation while tracking a force reference. This thesis employs a Hill/Huxley-type nonlinear model, developed by Ding et al. [9–11], to optimize stimulation trains in this manner. Another contribution of this research is that the ability to predict the muscle force resulting from an NMES pulse train is

not particularly useful in many clinical applications unless the force is controlled. Consider the application of NMES to perform a gripping task. In the absence of force control, NMES will provide no dexterity and a subject will be unable to effectively grip either a soft object or a rigid object. Additionally, it would be undesirable to grip a lighter object, such as a pencil, with the same force as a glass of water or heavier object. Excess fatigue induced in the muscle due to overstimulation seriously restricts many applications of NMES. This research applies optimization to maintain force at a controlled value.

4.0 THE HILL/HUXLEY-TYPE MODEL

The model discussed by Ding et al. in 2003 [11] was used to predict muscle response in this thesis. The model consists of 2 sets of differential equations that define a force model and a fatigue model. The force that the muscle generates is modeled as:

$$\frac{dC_N}{dt} = \frac{1}{\tau_c}\sum_{i=1}^{n} R_i \exp\left(-\frac{t-t_i}{\tau_c}\right) - \frac{C_N}{\tau_c},$$

$$R_i = 1 + (R_0 - 1)\exp[-(t_i - t_{i-1})/\tau_c], \tag{4.1}$$

$$\frac{dF}{dt} = A\frac{C_N}{K_m + C_N} - \frac{F}{\tau_1 + \tau_2\frac{C_N}{K_m+C_N}}.$$

The muscle fatigue is modeled as:

$$\frac{dA}{dt} = -\frac{A - A_{rest}}{\tau_{fat}} + \alpha_A F,$$

$$\frac{dKm}{dt} = -\frac{K_m - K_{m,rest}}{\tau_{fat}} + \alpha_{K_m} F, \tag{4.2}$$

$$\frac{d\tau_1}{dt} = -\frac{\tau_1 - \tau_{1,rest}}{\tau_{fat}} + \alpha_{\tau_1} F.$$

The parameters in 4.1 and 4.2 are defined in Table 2. Parameters sub-scripted "rest" in Equation 4.2 denote the parameter of the muscle when it is in a non-fatigued state. Note that Equation 4.2 is made up of a force-based component, F, and a recovery based component, τ_{fat}. The force based component predicts muscle fatigue, and the recovery based component predicts muscle recovery based on the state of the muscle. While attempting to reconstruct

this model using the muscle parameters identified in References [9–11], it was determined that although the force model would produce results comparable to those presented, the fatigue model produced unrealistic results, inconsistent with those presented. This was found to be due to misrepresentation of α_A in References [9–11] and of α_{τ_1} and α_{R_0} in References [9, 10]. Corrections to these model parameters are discussed in the Appendix.

Table 2: Definition of muscle model states and parameters (Adapted from [11])

Symbol	Definition
A	Scaling factor for the force and the shortening velocity of the muscle
C_N	Representation of Ca^{2+}-troponin complex
F	Instantaneous force
R_0	Mathematical term characterizing the magnitude of enhancement in C_N from the following stimuli
t_i	Time of the i^{th} stimulation
τ_1	Time constant of force decline at the absence of strongly bound cross-bridges
τ_2	Time constant of force decline due to the extra friction between actin and myosin resulting from the presence of cross-bridges.
K_m	Sensitivity of strongly bound cross-bridges to C_N
α_A	Coefficient for force-model parameter A in the fatigue model
α_{K_m}	Coefficient forK_m in the fatigue model
α_{τ_1}	Coefficient for force-model parameter τ_c in the fatigue model
τ_{fat}	Time constant controlling the recovery of the three force-model parameters (A, R_0, τ_c) during fatigue

5.0 EXPERIMENTAL SETUP

Experiments were conducted on a leg extension machine, shown in Fig. 3, fitted with a load cell aligned to measure isometric knee extension force. The load cell was placed 13 inches from the fulcrum of the knee. Straps were used to securely hold the subject's leg in place. The extension arm was locked in place such that the subject's knee angle was approximately 90 degrees. The quadriceps muscle was stimulated using an FNS-8 channel stimulator [CWE Inc., PA USA] to produce an isometric knee extension. Force was measured with a bidirectional force transducer. Early trials were performed with a U9C bidirectional force transducer [HBM Inc., Hesse, Germany]. Due to an equipment failure, later trials were performed using a LC101 model bidirectional force transducer [HBM Inc., Hesse, Germany](see Fig. 4). Both units were calibrated and gains defined appropriately to render force (N). Fig. 2 graphically depicts this test setup. Trials were performed on 4 healthy subjects, male, ages 20, 27 and 28. Data from the force transducer are collected using a Quanser Q8-US data acquisition board and is recorded using Simulink at a rate of 200 Hz. All data are filtered using a 12-order Butterworth filter with a normalized edge frequency of 0.2π radians per sample.

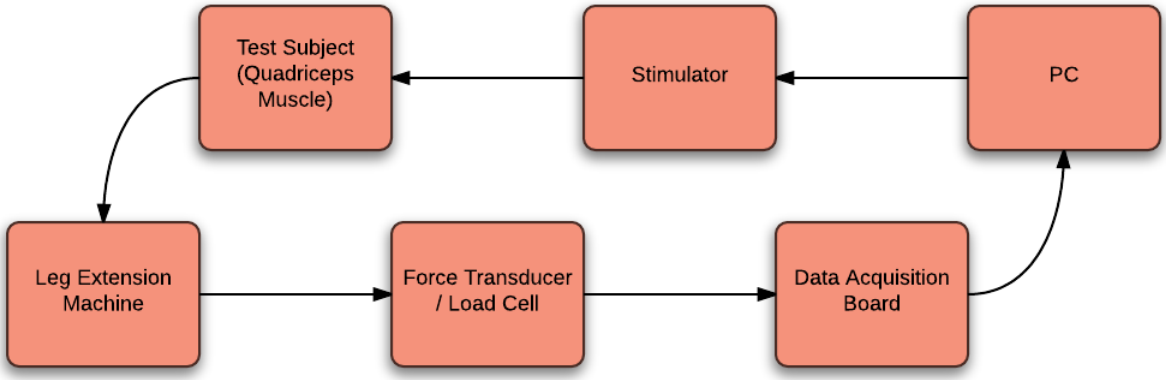

Figure 2: Flow chart of experimental setup

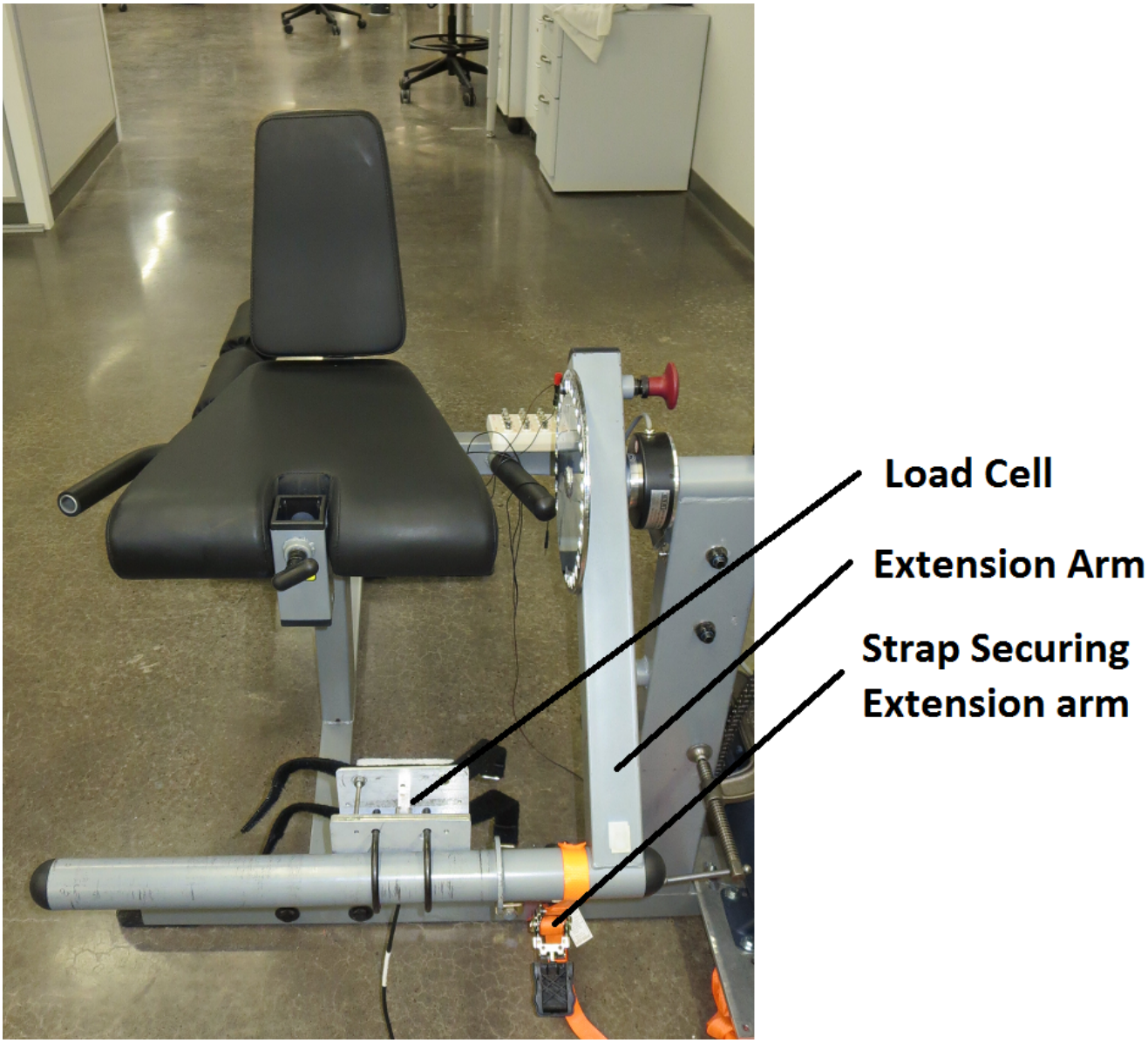

Figure 3: Leg extension machine with the extension arm locking into place and a load cell fitted to measure isometric knee extension force

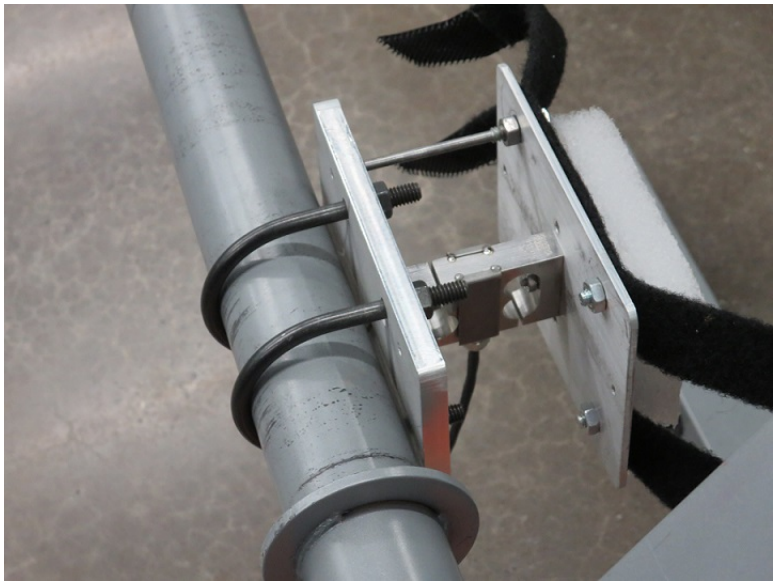

Figure 4: LC101 bidirectional force transducer fitted to the leg extension machine to measure isometric knee extension force

6.0 PARAMETER IDENTIFICATION

The parameter identification experiments performed on each of the test subjects, described in the following sections, are performed in a specific order to obtain the best muscle parameters and to maintain consistency between subjects throughout the experiments. Rest periods are applied between experiments to ensure that fatigued muscles are allowed ample time to recover. For all subjects, the same potentiation protocol (defined in detail in Section 6.2.1) is used and the rest period between the end of the potentiation protocol and the beginning of the data trial is maintained at 5 seconds. Each of these experiments is described in more detail in the following sections. Fig. 5 shows the process used in this thesis to conduct experiments and process data.

6.1 MAXIMUM VOLUNTARY ISOMETRIC CONTRACTION

The first experiment performed on each subject is to determine the Maximum Voluntary Isometric Contraction (MVIC) force. This term defines the maximum force that the subject can generate with the muscle in the absence of muscle stimulation. This determination is made in a similar manner to [11]. The subject is asked to perform a maximum voluntary contraction. To confirm the subject is producing maximum force, an 11 pulse (900 ns pulse width), 100 Hz stimulation is delivered during the contraction. If the measured force does not increase by more than 10%, the force is considered to be the MVIC force. After measuring MVIC, the stimulation current is adjusted such that a six pulse, 100 Hz pulse train produces a muscle force of approximately 20-30% of the MVIC magnitude. The muscle is then rested for 5 minutes.

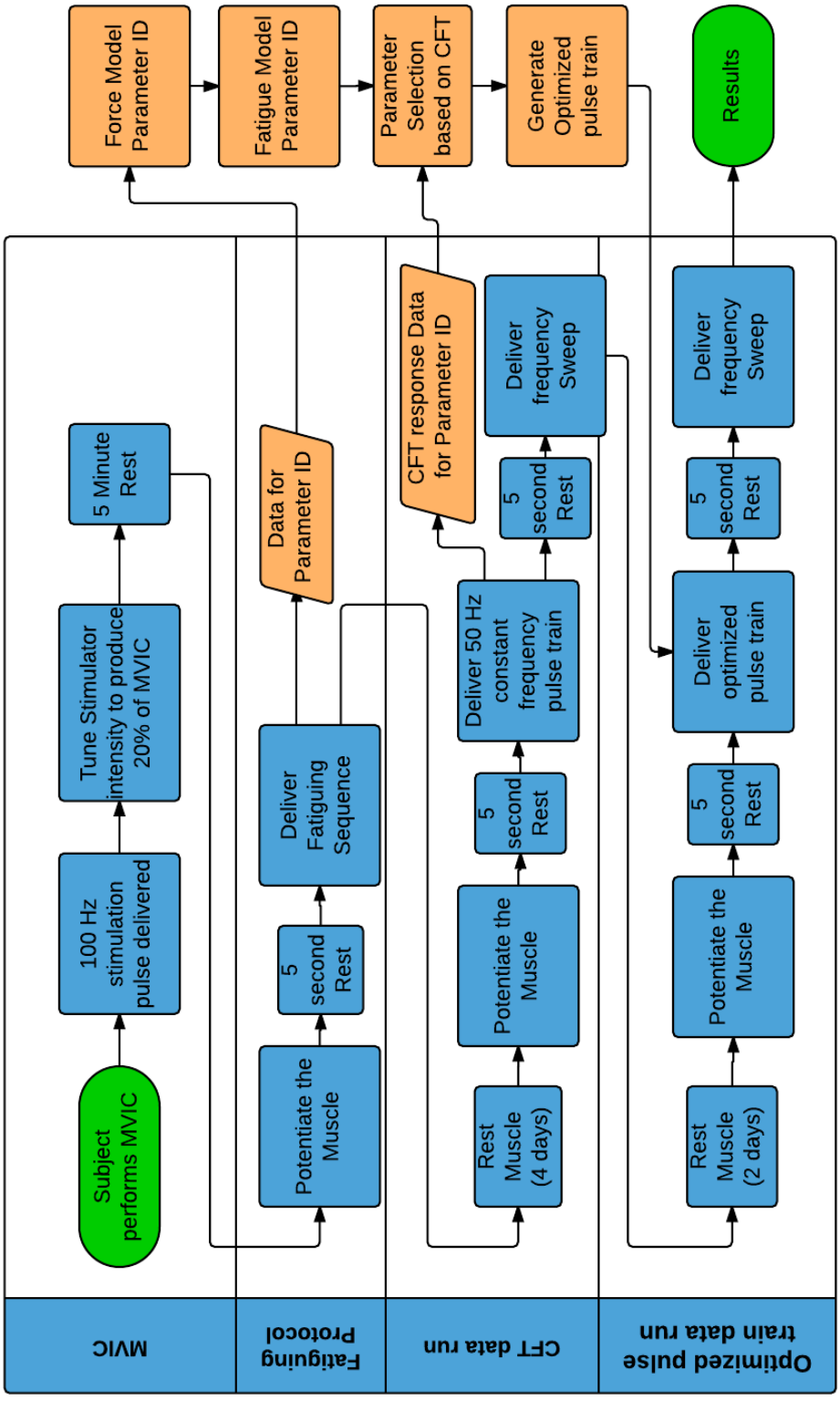

Figure 5: The flow of the experiments performed in this Thesis

The purpose of performing this experiment is to define a standardized pulse width and magnitude that will be used for the duration of testing. Unlike some other muscle models, the Ding et al. model does not account for change in stimulation magnitude. This means that if multiple stimulation magnitudes are to be used, the model parameters must be identified for each stimulation magnitude. The standardized pulse defined in this experiment will be used for all remaining experiments for a given subject.

6.2 FATIGUING PROTOCOL

The second experiment performed is the fatiguing protocol. The primary purpose of the fatiguing protocol is to identify the muscle parameters. During this experiment, the muscle is potentiated and then delivered a series of pulse trains to induce muscle fatigue.

6.2.1 Muscle Potentiation

Muscle potentiation, as it applies to NMES, is a practice where the muscle is delivered stimulation briefly in a manner such that the muscle does not fatigue significantly but is activated and prepared for further stimulation. This has been observed to result in more consistent muscle forces throughout the following pulse delivery and does not cause measurable muscle fatigue [10]. Muscle potentiation is performed prior to every fatiguing protocol. In addition to warming the muscle up, it also allows resulting muscle forces to be checked from day to day prior to beginning data trials. If potentiating peaks are significantly lower than a previous data collection, this could indicate that the muscle is fatigued or that the test equipment is not properly configured. In most cases, this can be resolved by simply reapplying the stimulation pads or rebooting the test equipment.

The muscle potentiation sequence used throughout the parameter identification experiments is a series of 35 800-ms 14 Hz CFT trains, where each train is composed of 12 pulses and spaced five seconds from the end of the previous train. Figure 6 shows an example of a 14 Hz CFT delivered during muscle potentiation. Muscle potentiation was followed by a 5 second rest period.

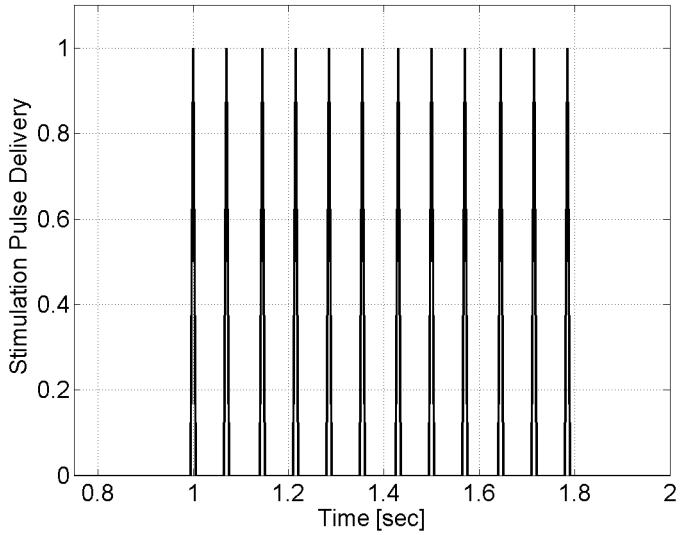

Figure 6: A plot of a 12 pulse, 14 Hz pulse train delivered to the muscle for the purpose of muscle potentiation. This train is delivered 35 times, 5 seconds apart during muscle potentiation

6.2.2 Fatiguing Sequence

The fatiguing sequence was intentionally designed to induce fatigue in the muscle and measure the forces generated by the muscle as it fatigues. This experiment collects the data necessary to identify muscle parameters for all parts of the muscle model. The fatiguing was performed using a pulse train sequence of a 20 pulse, 50 Hz CFT followed by a 14 pulse, 12.5 Hz VFT followed by 13, 33 pulse, 33 Hz CFT pulse trains. The series of pulse trains was repeated ten times to fatigue the muscle. The 33 Hz CFT was used because it was determined to be the most effective train for fatigue model parameter identification in [11].

The results of this experiment are passed into a sequence of data processing stages, as described in Section 6.3 to obtain multiple sets of possible muscle parameters. These sets are then compared against the result of the constant frequency datarun (Section 7.2) to identify which set performs best for the subject.

6.3 OPTIMIZATION FOR PARAMETER IDENTIFICATION

Model parameters were identified using the results of the fatiguing protocol in 2 stages. First, only the dynamics in 4.1 were modeled and the parameters for the non-fatigued muscle were identified using a mean-squared-error cost function. The function was evaluated over the first fatiguing series (first 15 pulse trains) because this is the region where the muscle is basically in an unfatigued state. The muscle fatigue induced by the first series of pulses is not significant as is evident by minimal change in magnitude of the muscle force, shown in Figs. 10 and 9. Calculating error over the first series provides a large enough dataset to account for variability in muscle response and equipment during measurement. This is a deviation from how parameters were identified in [11] but has been found to better address this variability. In the force parameter identification stage, the optimization tunes only A_{rest}, $\tau_{1,rest}$, τ_2, and $K_{m,rest}$ and the obtained optimal solution is recorded as the set of non-fatigued force model parameters.

Next, the fatigue dynamics in 4.2 were enabled in the model, and the optimization was repeated with all force parameters bounded at $\pm 10\%$ of the value obtained in the force parameter identification stage. All of the fatigue model parameters (α_A, α_{K_m}, α_{τ_1}, τ_{fat}) were set as free within reasonable bounds. This optimization was performed over the entire fatiguing protocol. The time constant of the calcium dynamics, τ_c, is set to 20ms, which is consistent with [8–11], and is identified throughout as sufficient for human quadriceps muscles in various states of fatigue. This value represents the time constant of the calcium dynamics, C_N, which is a chemical reaction and should be approximately the same for all subjects. It should be noted that the identified parameters for this model are specific to the magnitude of the standardized pulse, the muscle properties of the test subject, size and

placement of the stimulation pads, and placement of the load cell on the subject's shank. The parametrized muscle model for the test subject, plotted with the load cell data used to perform the parameter identification, is shown in Figs. 10 and 9.

All parameter identification optimizations were performed using the optimization toolbox, *fmincon* (MATLAB, USA). Due to the non-linear nature of the model, it was expected that the optimization algorithm may render a local minimum as a solution. To avoid local minimums, each stage of the optimization was performed multiple times beginning at unique, randomized starting points. The force parameter optimization was performed 100 times per dataset. The five lowest cost force parameter sets were then used for fatigue parameter identification. All five fatigue parameter sets were compared to the CFT data run. The set with the best match was recorded as the identified parameter set. This process ensures that the modeled prediction adequately fits the measured force data.

6.4 MODEL PARAMETER IDENTIFICATION RESULTS

Model parameter identification is initially performed for only the force model parameters. These parameters are A_{rest}, $\tau_{1,rest}$, τ_2, and $K_{m,rest}$. The identification process involves disabling the fatigue model and minimizing error between the predicted and measured force. Figs. 7(a) and 7(b) show the result of the force parameter identification. Note that spikes are observed in some force data at the onset of each pulse. This appears to be linked to the load cell used to measure the force. This effect can be clearly seen in Figs. 8(a) and 8(b) at the beginning of the fatiguing protocol. The affect also appears to be more visable in subjects who have been not been stimulated regularly with NMES. Although this results in

an unpredicted spike in the data, and therefore yields slightly larger error between modeled and predicted in the parameter identification. The resulting identified parameters are not significantly affected because the prediction is optimized to the force once it stabilizes. Force model parameters are identified my minimizing the following cost function of the error, ε_{RMS}:

$$\varepsilon_{RMS} = \sqrt{\frac{1}{N}\sum_{n=0}^{N}\left(F_p[n;u] - F_m[n;u]\right)^2};\ u = t_1, t_2, \cdots, t_k, \tag{6.1}$$

Subject to the dynamic constraints implicit in ε_{RMS} where ε_{RMS} is the RMS error incurred by the system, F_p is the force predicted for a pulses in the fatiguing sequence, u, by (4.1) and (4.2) at sample n, F_m is the measured force during the fatiguing protocol.

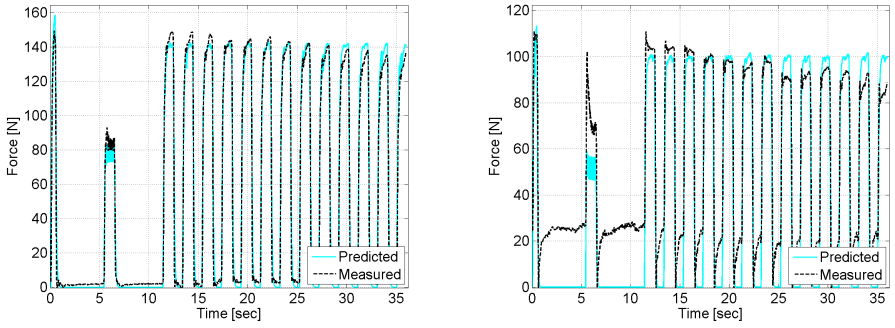

Figure 7: Non-fatigued parameter identification. Note that non-fatigued parameter identification is only performed using the first 15 pulse trains of the fatiguing protocol. After this point, the muscle has fatigued such that the force magnitudes are not accurate for parameter identification.

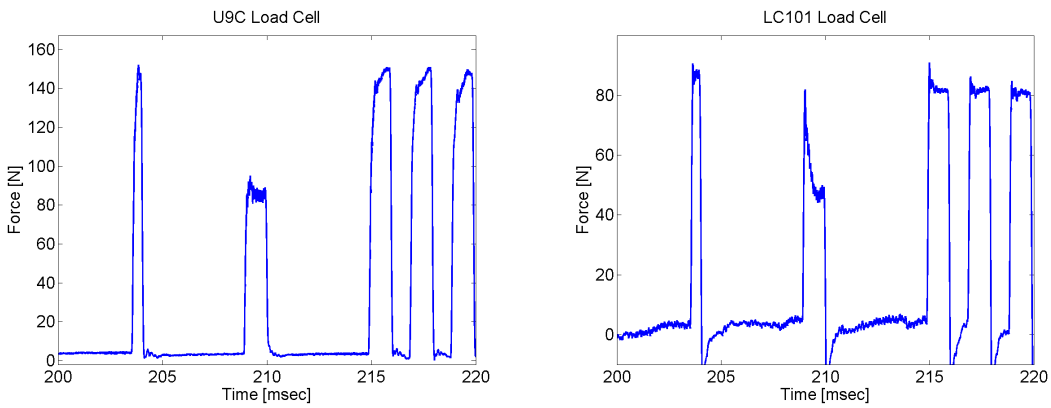

Figure 8: Comparison of force spikes by load cell.

Following non-fatigued model parameter identification, fatigue parameter identification was performed. During this process, non-fatigued model parameters were bounded at ±10%. The fatigue model parameters (α_A, α_{K_m}, α_{τ_1}, and τ_{fat}) were set as free within reasonable bounds. Figs. 10 and 9 show the result of the fatigue parameter identification. Table 4 lists the non-fatigued parameters obtained for all test subjects. In some cases, during the fatiguing protocol, the muscle exhibits a property where force does not decay to near zero between pulse trains. This is shown in Fig. 9. In my testing, this affect has only been observed at higher stimulation magnitudes. The force model (4.1) does not have a way to compensate for this, but the identified parameters do otherwise fit the model appropriately. Performance of these parameters in the optimization is evaluated in Table 3.

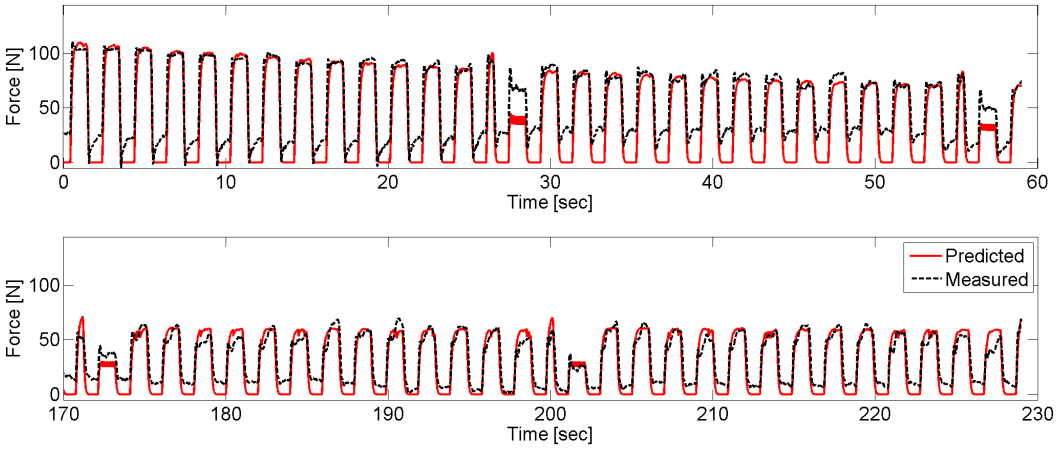

Figure 9: Subject 1 fatigued parameter identification.

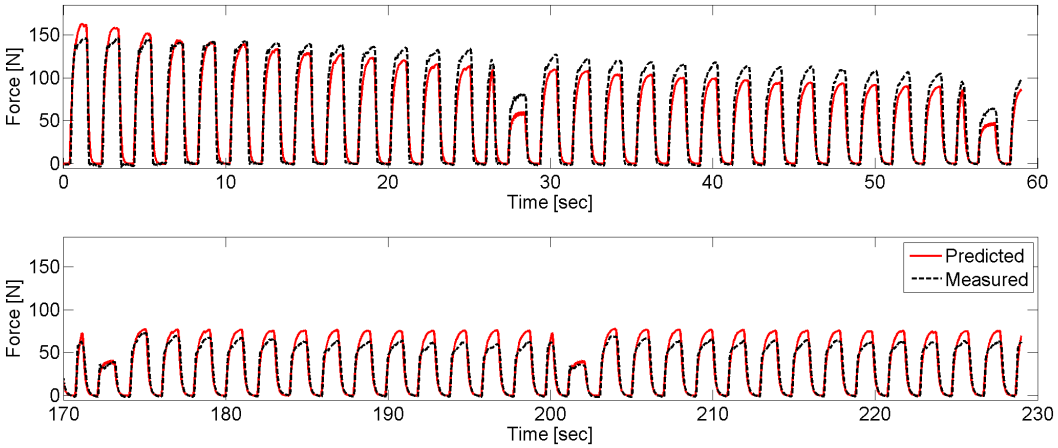

Figure 10: Subject 3 fatigued parameter identification.

Table 3: Root-mean-square error of fatigue parameter identification

Subject 1	Subject 2	Subject 3	Subject 4
13.52 N	6.21 N	5.59 N	13.79 N

Table 4: Model parameters for fatigued muscle parameter identification. Note that this also includes the force model parameters that were bounded at ±10% of the parameters identified for the non-fatigued state.

	Units	Subject 1	Subject 2	Subject 3	Subject 4
τ_2	ms	46.39	47.76	44.00	43.48
$\tau_{1,rest}$	ms	18.56	18.15	16.50	36.63
A_{rest}	N/ms	2.64	1.60	4.30	1.95
$K_{m,rest}$	-	0.23	0.18	0.18	0.26
α_{τ_1}	N^{-1}	2.00×10^{-5}	2.05×10^{-6}	2.93×10^{-6}	2.00×10^{-6}
α_A	ms^{-2}	-7.06×10^{-7}	-7.95×10^{-7}	-8.00×10^{-7}	-7.70×10^{-7}
α_{K_m}	$ms^{-1}N^{-1}$	4.52×10^{-8}	8.33×10^{-8}	4.13×10^{-8}	4.07×10^{-8}
τ_{fat}	s	95.47	68.83	66.16	68.24

7.0 OPTIMIZATION OF PULSE TRAIN

This section discusses the calculation of the optimized pulse train and compares the performance of the optimized train to a constant frequency train. Each of these experiments is described in more detail in the following sections. Consistency is particularly important when performing the CFT data run (Section 7.2) and the optimized pulse train data run (Section 7.4) because the results of these runs are compared as part of the conclusion that an optimized pulse train results in less muscle fatigue than a comparable constant frequency train. Misplacement of the stimulation pads or other experimental variations can reduce the magnitude of the delivered stimulation and cause the forces magnitudes to differ. This prevents comparison of the results. Particular care was taken to collect this data in a consistent manner and force magnitudes were checked using initial test pulses prior to recording data.

7.1 MUSCLE POTENTIATION

Muscle potentiation is performed prior to the CFT data run (Section 7.2) and optimized pulse train data run (Section 7.4). The muscle potentiation sequence used in these experiments is a series of 35 800-ms 14 Hz CFT trains, where each train is composed of 12 pulses and spaced five seconds from the end of the previous train.

7.2 CONSTANT FREQUENCY DATA RUN

The third experiment in this thesis is the constant frequency data run. This experiment collects data while stimulating the muscle with a 30 second, 50 Hz CFT. The muscle was potentiated prior to the CFT followed by a 5 second rest period. The 30 second CFT was then delivered to the muscle. Five seconds after the 50Hz CFT train, the muscle was delivered a series of five second CFTs with frequency of each train increasing by 10 Hz from 30 Hz to 100 Hz. This was done to assess the level of fatigue in the muscle as described in Section 7.5.

The results of this experiment are used to assess which of the sets of muscle parameters best predicts the response of the muscle to the 50 Hz CFT. This is done by evaluating a cost function based on the error between the measured result and the result predicted for the 50 Hz pulse train by each of the sets of muscle parameters. Additionally, these data are used to evaluate the force-time integral of the muscle response. This number is used to calculate an appropriate force reference for the optimized pulse train such that the integral of the force is the same for 50 Hz CFT and the prediction of optimized train, described in the final experiment.

7.3 OPTIMIZED PULSE TRAIN CALCULATION

The objective of this calculation was to compute an optimized pulse train to track a force reference. The optimization toolbox, *fmincon* (MATLAB, USA), was used to compute the optimized stimulation train. The optimization problem was to define the optimal series of stimulation pulse times to minimize the error between the predicted force and force reference and minimize the number of pulses delivered. Mathematically, this cost function is defined as follows:

Find an optimal sequence of stimulation pulses, u, to minimize:

$$C = \frac{1}{T}\int_0^T \left(F_p(\tau; u) - F_r\right)^2 d\tau + Lk;\ u = t_1, t_2, \cdots, t_k, \tag{7.1}$$

subject to:

$$t_i - t_{i-1} > 10 \text{ ms } \forall i = 1, \cdots, k\ , \tag{7.2}$$

and the dynamic constraints implicit in C where C is the cost incurred by the system, F_p is the force predicted for a sequence of stimulation pulses, u, by (4.1) and (4.2) at time τ, F_r is the reference (or desired) force, k is the number of pulses delivered to the muscle over the sampling period, and L is a weighting factor of k.

The constraint in 7.2 limits the time between pulses to be greater than 10ms, which imposes an upper limit on the stimulation frequency of 100 Hz. The upper limit of the stimulator is 200 Hz, but stimulation at higher frequencies has been shown to fatigue muscles more quickly. This, therefore, contributes to a reduction in muscle fatigue.

Since u is a k x 1 matrix, this poses the problem of solving an optimization based on a variable number of inputs. The term k is both an input to the optimization and the definition of the number of terms in u, which is also an input. This problem is addressed by performing the optimization over a longer time period (60-seconds) and only evaluating the cost function over the first 30-seconds. The optimization will shift pulses into or out of the observed region as needed to minimize the cost function. The value of k is then defined to be the number of pulses in the pulse train that remain in the 30-second observed region. This effectively assigns zero cost to any force generated outside of the observed region and minimizes the number of pulses in the region. The discrete time implementation of the cost function in MATLAB is as stated in Equation (7.3).

Find an optimal sequence of stimulation pulses that minimize:

$$C = \frac{1}{N}\sum_{n=0}^{N} \left(F_p[n;u] - F_r\right)^2 + Lk;\ u = t_1, t_2, \cdots, t_k, \tag{7.3}$$

subject to:

$$t_i - t_{i-1} > 10 \text{ ms } \forall i = 1, \cdots, g\ , \tag{7.4}$$

$$t_k < \ 30 \text{ sec}, \tag{7.5}$$

$$t_{k+1} > \ 30 \text{ sec}, \tag{7.6}$$

$$t_i < \ 60 \text{ sec } \forall i = 1, \cdots, g \tag{7.7}$$

and the dynamic constraints implicit in C where g is a user defined number of pulses, n is the sample number, and N is the last sample.

7.4 OPTIMIZED PULSE TRAIN DATA RUN

The final experiment is the optimized pulse train data run. The pulses delivered in this data run are calculated based on the muscle parameters identified using the data from the previous experiments. Using the optimization scheme discussed in Section 7.3, the pulse train is identified to induce less muscle fatigue while producing approximately the same force-time integral. The optimized run is a form of open-loop control where an input pulse train is designed such that predicted output force will track a reference. Accuracy of the output is entirely based on the accuracy of the model because the system has no ability to account for error. The frequency sweep, applied to the muscle at the end of this experiment will be used to compare the level of fatigue of the muscle following the optimized pulse train data run to the CFT data run. This comparison is described in more detail in Section 7.5.

7.5 FREQUENCY SWEEP FOLLOWING EACH DATA RUN

Five seconds after the optimization train and the constant frequency train, the muscle is delivered a series of five second CFTs, with frequency of each train increasing by 10 Hz from 30 Hz to 100 Hz. The purpose of this is to stimulate the muscle in such a way that the maximum force is identified for the muscle in the current state. Based on Equation (4.1), the calcium dynamics, which are directly related to muscle fatigue, affect the magnitude of force generation. Since unfatigued muscle parameters are unchanged, the magnitude of the force produced by the muscle can be directly compared to assess muscle fatigue. The peak force and force-time integrals of the frequency sweep will be compared to identify fatigued state of the muscle following delivery of optimization train and the constant frequency train.

7.6 OPTIMIZED PULSE TRAIN RESULTS

The optimized pulse train is defined by minimizing the cost function defined in 7.3. As predicted muscle fatigue increase, the optimization will increase the rate of the stimulation in an attempt to compensate. The 20-sample moving average frequency of the optimized pulse train is depicted in Fig. 11. The muscle stimulator is provided stimulation times at a 5-µs time steps, so this limits stimulation pulse times to multiples of 5-µs. Predicted muscle response to the optimized pulse train is plotted with the measured results in Fig. 12. It is important to note that due to modeling inaccuracy and the open-loop nature of the system, error is expected. Lack of a feedback loop means that error at any point in the trial will propagate throughout the remainder of the trial. Also note that the model predicts much more fluctuation about the reference than was observed in the measured data. The measured data was filtered to reduce load cell noise, which may explain the absence of the high frequency components.

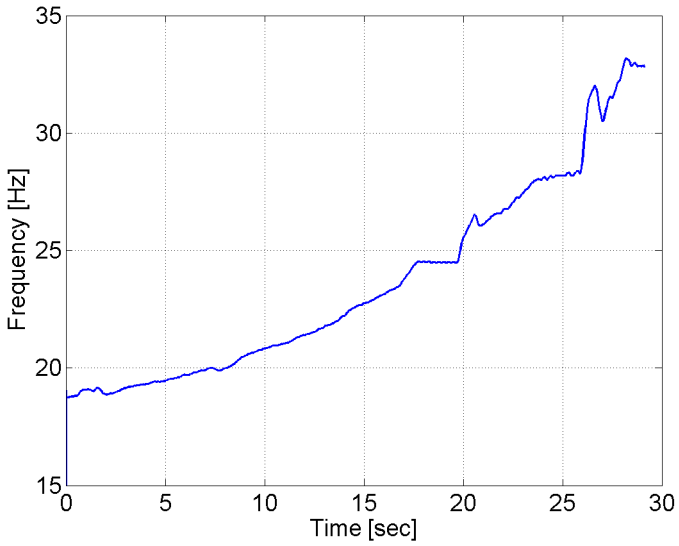

Figure 11: 20-sample moving average of frequency of optimized stimulation pulse train

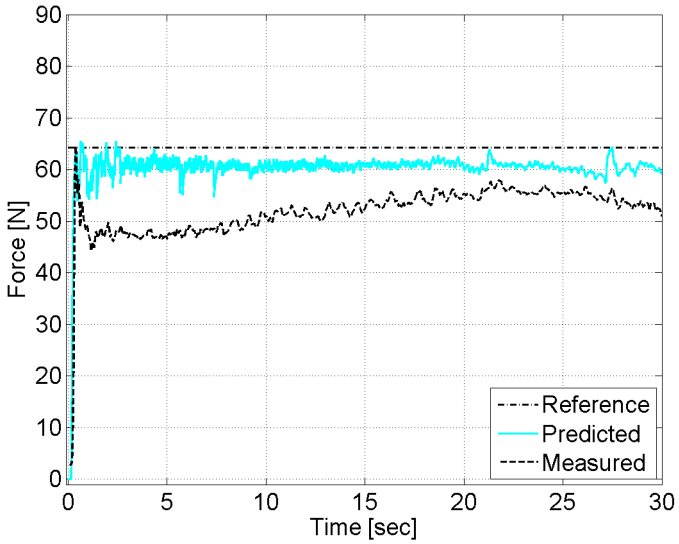

Figure 12: The predicted force response of the optimized train vs. measured response. The pulse train tracks the force reference with some noticeable error.

7.7 ANALYSIS OF MUSCLE FATIGUE FOLLOWING STIMULATION

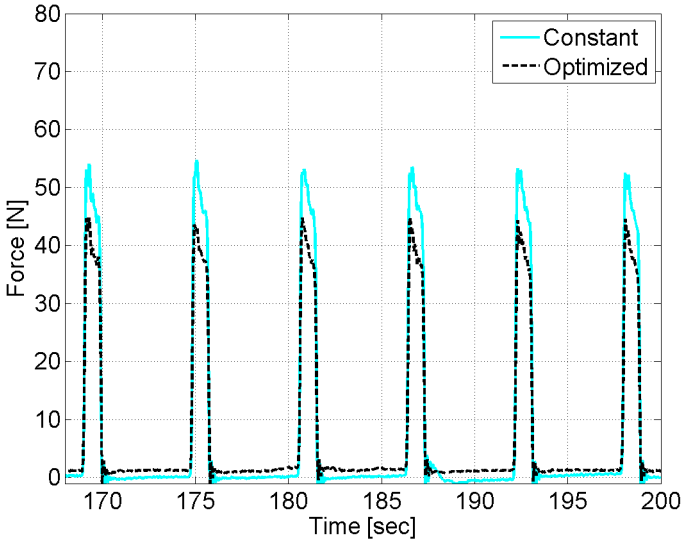

Figure 13: The force resulting from the final potentiation pulses, applied just before delivering the optimized and constant frequency trains, are shown to be of comparable amplitude.

The force resulting from the final potentiation pulses, applied just before delivering the optimized and constant frequency trains, are shown in Fig. 13 to be of comparable amplitude. This indicates that the level of fatigue in the muscle prior to the CFT data run (Section 7.2) and the optimized pulse train data run (Section 7.4) are comparable. This supports the conclusion by confirming that the muscle was not more fatigued prior to one datarun than the other.

Five seconds after the optimization train and the constant frequency train, the frequency sweep is delivered (Section 7.5). The results of this show a notable improvement in peak magnitude of the force in all cases. The resulting force response for both trials is shown for 1 subject in Fig. 14. The results for both subjects are shown in Table 5. These results suggests that the muscle is more fatigued following delivery of a constant frequency train than when stimulated with the offline computed, optimized pulse train.

To determine whether fatigue was substantially reduced for the optimized trial, the state of the muscle is compared to the state following a 50-Hz CFT. As discussed in Section 7.5, this is done by delivering a series of CFTs to the muscle with frequency of each train increasing by 10 Hz from 30 Hz to 100 Hz. The peak force generated in these trials demonstrates that muscle fatigue is reduced.

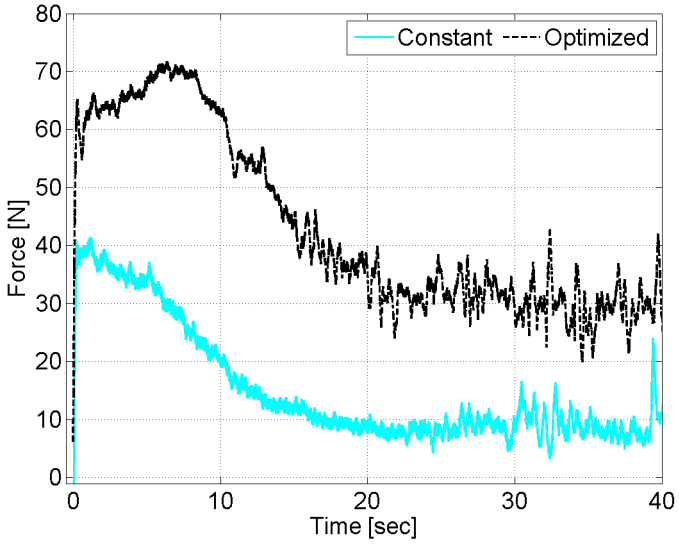

Figure 14: Muscle response to the frequency ramp following the 30-second CFT and optimized dataruns. As identified in Table 5, the force-time integral and the peak force were calculated to be higher for the optimized train.

Table 5: Characteristics of frequency sweep trials - Peak Force P-value= 0.046 F-t Integral P-value= 0.217. This indicates that the peak force is statistically significant for this dataset.

Parameter	Subject 1	Subject 2	Subject 3	Subject 4
Optimized train Peak Force	87.66 N	48.94 N	96.94 N	140.98 N
CFT Peak Force	69.59 N	40.40 N	58.92 N	134.78 N
Optimized train F-t Integral	64.72 $N \cdot s$	24.43 $N \cdot s$	52.99 $N \cdot s$	92.61 $N \cdot s$
CFT F-t Integral	48.06 $N \cdot s$	18.10 $N \cdot s$	43.91$N \cdot s$	103.62 $N \cdot s$

8.0 CONCLUSION

This thesis has examined a Hill/Huxley-type force and fatigue model of the human skeletal muscle. The model was implemented in an open-loop control scheme that optimizes an NMES pulse train to limit muscle fatigue while controlling an isometric contraction to a force. Implementation of the model involved identifying muscle parameters for each subject, calculating the optimized pulse train, and comparing the fatigue induced by the optimized train to that of a CFT. Since fatigue is commonly a limitation in clinical applications of NMES, the investigations of this thesis are particularly relevant to common NMES applications such as drop foot correction or NMES assisted grasping, bladder control, standing or balance tasks. In addition to fatigue management, this thesis demonstrates a method of model based force control that could be used to avoid overstimulation of the muscle in clinical applications, and therefore slow the onset of muscle fatigue.

This thesis found that the presented model sufficiently predicted muscle force response to a 30-second optimized pulse train. It has also concluded that the presented muscle parameter identification techniques were sufficient to identify muscle parameters for use in a model-based system. The results have confirmed that the previously published model, implemented in a model-based optimizer is capable of calculating an optimized pulse train that will reduce muscle fatigue in NMES applications. This thesis takes a small step to improve implantations of NMES and thereby improve quality of life for people who rely on NMES due to injury, disorders, stroke, or muscle related impairments.

9.0 FUTURE WORK

This research has set the stage for further advances and improvements to expand the model to more complex applications. Implementation of a model-based, closed loop control system to maintain muscle force and account for error is an achievable goal. Additionally, expanding the model to account for multiple joint angles for dynamic applications is another area of interest. Investigation into the use of the model at multiple stimulation magnitudes would present a new control problem that would further expand the model but potentially reduce muscle fatigue or offer other efficiencies. These enhancements will further expand the usability of the model for implementation in neuroprothesies or other clinical applications of NMES.

APPENDIX

CORRECTION TO DING ET AL. MODEL

Through the process of modeling the results described in [9–11], I've determined that the parameter α_A in [9–11] and the parameters α_{τ_1} and α_{R_0} in [9,10] were incorrectly reported. I initially made this determination by individually disabling each of the differential equations in Equation 4.2 and observing the resulting model output. This did not entirely expose the problem, so I proceeded to disable either the recovery or the force-based terms of Equation 4.2. By setting α_A, α_{K_m}, and α_{τ_1} to zero, it became evident that the incorrectly reported terms were in the fatigue/force-based portion of the model. It should be noted that disabling the force-based terms inherently sets the recovery term to zero because it does not induce any change in the recovery states (they will stay at the resting values). To understand how modeled muscle recovery will look in the absence of muscle fatigue, the initial state of the model must be set to something other than the resting state so that the model has something to converge to and does start in an already converged state.

I corrected these parameters in my simulations to produce feasible knee extension forces. I discussed this finding with Dr. Susan Marion of the Department of Physical Therapy at University of Delaware who acknowledged my viewpoint and assisted me by providing their corrected parameters for use in my model. Dr. Marion is a colleague of Dr. Wexler and Dr. Binder-Macleod (Both authors of [8–12]).

Table 6: This table lists model parameters identified in the published models that vary significantly from the parameters obtained in my testing.

	Parameter	
	α_A [ms^{-2}]	α_{τ_1} [N^{-1}]
[11]	-40	2.1×10^{-5} *
[9]	-0.047	0.306
[10]	-0.056	0.306
Corrected	-4.0×10^{-7}	2.1×10^{-5}

*Note that this parameter did not need to be corrected but is included here for completeness

Parameters α_A and α_{τ_1} are used in the Equation 4.2 of this thesis, and are defined in Table 2. The original muscle parameters from [9–11] are identified in Table 6. Using the corrected parameters, the predicted muscle response was observed to be consistent with the figures presented in [11]. Figures 15-18 show the force response and state values of the model using the parameters published in [11] and corrected parameters in a simulated trial.

In the model presented in [9, 10], K_m is a constant parameter and R_0 is modeled to change with fatigue. Although R_0 is a constant parameter in this thesis, it should be noted that α_{R_0}, which is the coefficient of R_0, is also incorrectly stated in [9, 10]. Works published prior to [9, 10] could also exhibit similar errors to those identified here. A brief review of related references identifies that the parameters published in [8] are also out of line with the corrected parameters identified here.

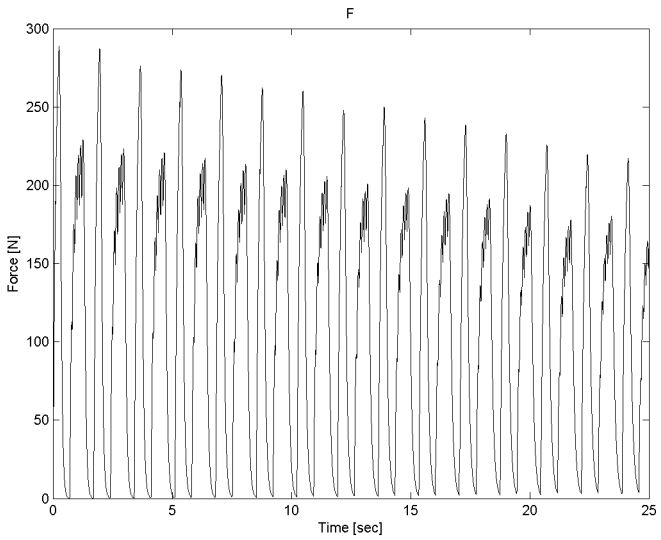

Figure 15: Predicted muscle force response using the corrected parameters

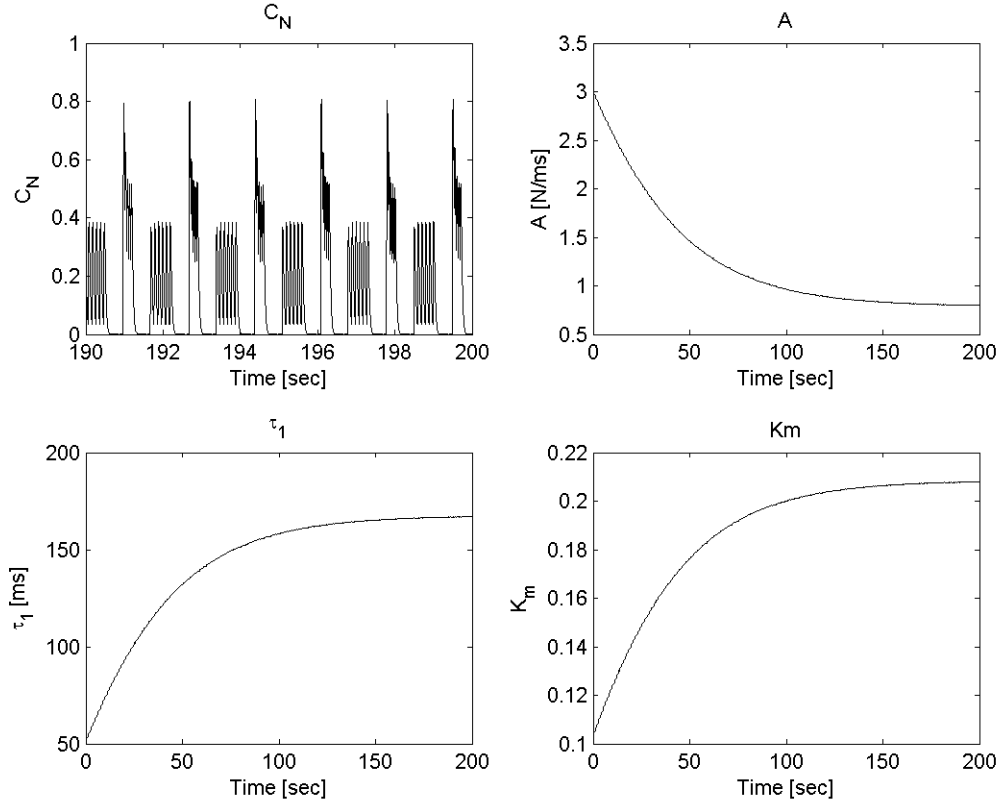

Figure 16: Muscle parameter states of the model using the corrected parameters

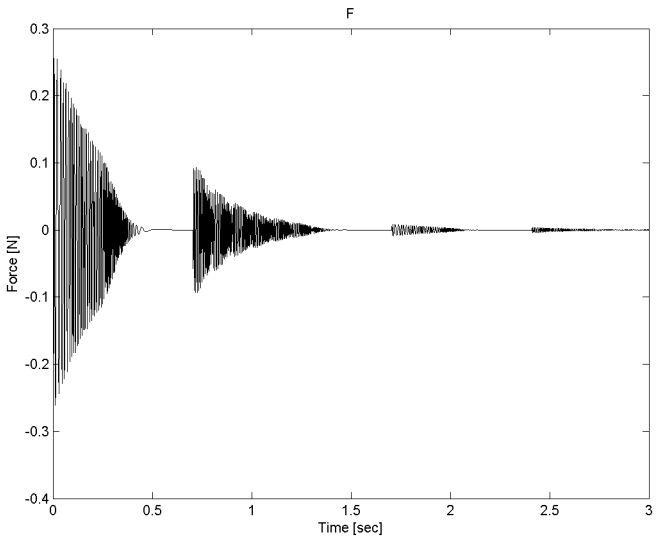

Figure 17: Predicted muscle force response using the published parameters

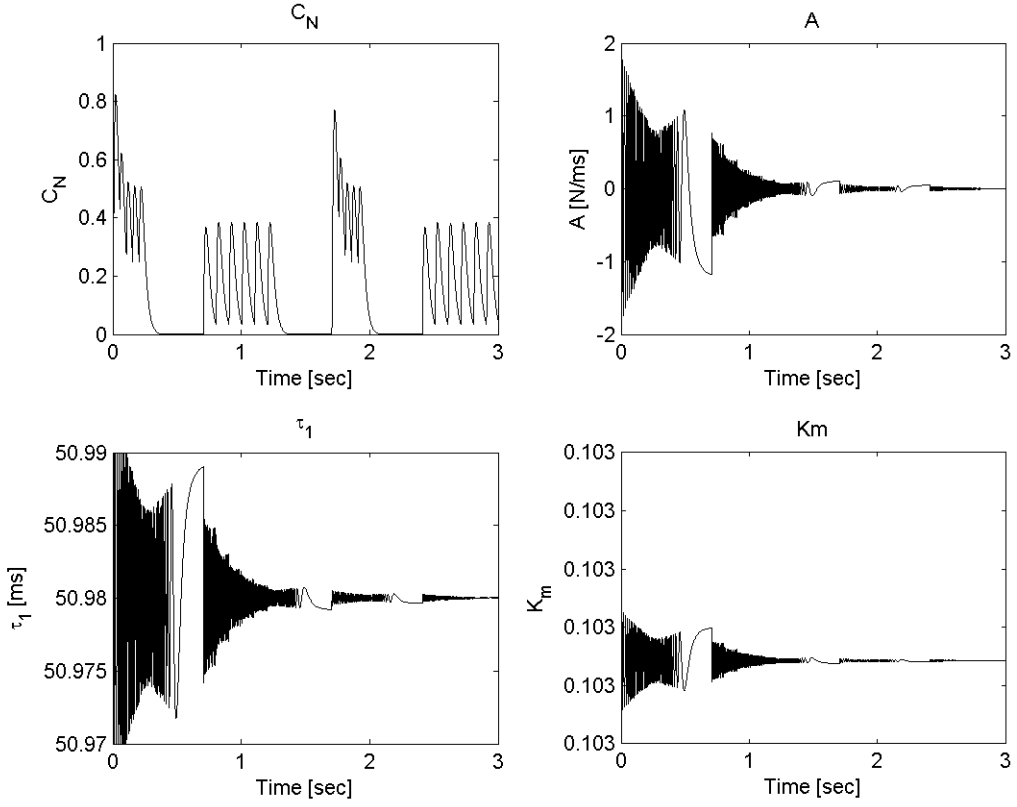

Figure 18: Muscle parameter states of the model using the published parameters

BIBLIOGRAPHY

[1] D. G. Allen, G. D. Lamb, and H. Westerblad. Skeletal muscle fatigue: Cellular mechanism. *Physiological Reviews*, 88:287–332, 2008.

[2] Martin W. Berchtold, Heinrich Brinkmeier, and Markus Mntener. Calcium ion in skeletal muscle: Its crucial role for muscle function, plasticity, and disease. *Physiological Reviews*, 80:1215–, 2000.

[3] L. A. Bernotas, P. E. Crago, and H. J. Chizeck. A discrete–time model of electrically stimulated muscle. *IEEE Trans. on Biomedical Engineering*, 33:829–838, 1986.

[4] C Scott Bickel, Chris M Gregory, and Jesse C Dean. Motor unit recruitment during neuromuscular electrical stimulation: a critical appraisal. *European journal of applied physiology*, 111(10):2399–2407, 2011.

[5] Jacques Bobet and Richard B Stein. A simple model of force generation by skeletal muscle during dynamic isometric contractions. *Biomedical Engineering, IEEE Transactions on*, 45(8):1010–1016, 1998.

[6] Lucy J. Colwell and Michael P. Brenner. Action potential initiation in the hodgkin-huxley model. *PLoS Comput Biol.*, 5, 2009.

[7] J. Ding, A. Wexler, and S. Binder-Macleod. Two-step, predictive, isometric force model tested on data from human and rat muscles. *J. Appl. Physiol.*, 85:2176–2189, 1998.

[8] J. Ding, A. Wexler, and S. Binder-Macleod. A predictive model of fatigue in human skeletal muscles. *Journal of applied physiology (Bethesda, Md. : 1985)*, 89:1322–1332, 2000.

[9] J. Ding, A. Wexler, and S. Binder-Macleod. A predictive fatigue model–I: Predicting the effect of stimulation frequency and pattern on fatigue. *IEEE Transactions on Neural Systems and Rehabilitation Engineering*, 10:48–58, 2002.

[10] J. Ding, A. Wexler, and S. Binder-Macleod. A predictive fatigue model–II: Predicting the effect of resting times on fatigue. *IEEE Transactions on Neural Systems and Rehabilitation Engineering*, 10:59–67, 2002.

[11] J. Ding, A. Wexler, and S. Binder-Macleod. Mathematical models for fatigue minimization during functional electrical stimulation. *Journal of Electromyography and Kinesiology*, 13:575–588, 2003.

[12] J. Ding, A. S. Wexler, and S. A. Binder-Macleod. Development of a mathematical model that predicts optimal muscle activation patterns by using brief trains. *Journal of Applied Physiology*, 88(3):917–925, 2000.

[13] S. J. Dorgan and M. J. O'Malley. A nonlinear mathematical model of electrically stimulated skeletal muscle. *IEEE Trans Rehabil Eng.*, 5:179–194, 1997.

[14] A. V. Hill. The heat of shortening and the dynamic constants of muscle. *Proceedings of the Royal Society of London B: Biological Sciences*, 126:136–195, 1938.

[15] A. L. Hodgkin and A. F. Huxley. Resting and action potentials in single nerve fibers. *The Journal of Physiology*, 104:176–195, 1945.

[16] A. L. Hodgkin and A. F. Huxley. A quantitative description of membrane current and its application to conduction and excitation in nerve. *J Physiol.*, 117:500–544, 1952.

[17] A. Krajl, T. Bajd, R. Turk, and H. Benko. Posture switching for prolonging functional electrical stimulation standing in paraplegic patients. *Paraplegia*, 24:221, 1986.

[18] Laura A Frey Law and Richard K Shields. Predicting human chronically paralyzed muscle force: a comparison of three mathematical models. *Journal of applied physiology*, 100(3):1027–1036, 2006.

[19] W. T. Liberson, H. J. Holmquest, D. Scot, and M. Dow. Functional electrotherapy: stimulation of the peroneal nerve synchronized with the swing phase of the gait of hemiplegic patients. *Arch Phys Med Rehabil*, 42:101–105, 1961.

[20] Gerard M Lyons, Thomas Sinkjær, Jane H Burridge, and David J Wilcox. A review of portable FES-based neural orthoses for the correction of drop foot. *IEEE Transactions on Neural Systems and Rehabilitation Engineering*, 10(4):260–279, 2002.

[21] E. Marsolais and R. Kobetic. Functional electrical stimulation for walking in paraplegia. *The Journal of Bone and Joint Surgery*, 69(5):728–733, 1987.

[22] J. H. Moe and H. W. Post. Functional electrical stimulation for ambulation in hemiplegia. *J Lancet*, 82:285–288, 1962.

[23] C. A. Phillips, J. S. Petrofsky, D. M. Hendershot, and D. Stafford. Functional electrical exercise: a comprehensive approach for physical conditioning of the spinal cord injured patient. *Orthopedics*, 7:1112–1123, 1984.

[24] Dejan B Popovic, Mirjana B Popovic, Thomas Sinkjaer, Aleksandra Stefanovic, and Laszlo Schwirtlich. Therapy of paretic arm in hemiplegic subjects augmented with a

neural prosthesis: A cross-over study. *Canadian Journal of Physiology and Pharmacology*, 82(8-9):749–756, 2004. PMID: 15523532.

[25] Arthur Prochazka, Michel Gauthier, Marguerite Wieler, and Zoltan Kenwell. The bionic glove: An electrical stimulator garment that provides controlled grasp and hand opening in quadriplegia. *Archives of Physical Medicine and Rehabilitation*, 78(6):608 – 614, 1997.

[26] B. Smith, Zhengnian Tang, M.W. Johnson, S. Pourmehdi, M.M. Gazdik, J.R. Buckett, and P.H. Peckham. An externally powered, multichannel, implantable stimulator-telemeter for control of paralyzed muscle. *Biomedical Engineering, IEEE Transactions on*, 45(4):463–475, April 1998.

[27] M. Solomonow, R. Baratta, H. Shoji, M. Ichie, S. Hwang, N. Rightor, W. Walker, R. Douglas, and R. D'Ambrosia. FES powered locomotion of paraplegics fitted with the LSU reciprocating gait orthoses (RGO). In *Annual International Conference of the IEEE Engineering in Medicine and Biology Society*, volume 4, page 1672, 1988.

[28] Ronald J. Triolo, Carol Bieri, James Uhlir, Rudi Kobetic, Avram Scheiner, and E.Byron Marsolais. Implanted functional neuromuscular stimulation systems for individuals with cervical spinal cord injuries: Clinical case reports. *Archives of Physical Medicine and Rehabilitation*, 77(11):1119 – 1128, 1996.

[29] J. Wexler, A. Ding and S. Binder-Macleod. A mathematical model that predicts skeletal muscle force. *IEEE TRANSACTIONS ON BIOMEDICAL ENGINEERING*, 44:337–348, 1997.

[30] P. M. Zoll. Resuscitation of the heart in ventricular standstill by external electric stimulation. *The New England Journal of Medicine*, 247:768–771, 1952.